

## Elastic $s$ -wave scattering phase shifts and $|V_{ub}|$ from lattice calculations of form factors for exclusive semileptonic decays

---

**J.M. Flynn\***

*University of Southampton, UK*

*E-mail: jflynn@phys.soton.ac.uk*

**J. Nieves**

*Universidad de Granada, Spain*

*E-mail: jmnieves@ugr.es*

Omnès dispersion relations make a connection between form factors for exclusive semileptonic decays and phase shifts in the corresponding elastic scattering channels. We describe two applications. In the first, we use lattice form factor calculations to learn about phase shifts in elastic  $s$ -wave isospin-1/2 channels for  $K\pi$ ,  $B\pi$ ,  $D\pi$  and  $DK$  scattering. The aim of the second application is to make the determination of the CKM matrix element magnitude  $|V_{ub}|$  from exclusive semileptonic  $B \rightarrow \pi$  decays competitive with that from inclusive decays. Here we use many subtractions in an Omnès dispersion relation to motivate a simple fitting function, allowing data to constrain the  $q^2$  shape of the differential decay rate and theory, primarily lattice results, to provide normalisation via form factor values.

*The XXV International Symposium on Lattice Field Theory*

*July 30 – August 4 2007*

*Regensburg, Germany*

---

\*Speaker.

## 1. Omnès dispersion relations

Mandelstam's hypothesis of maximum analyticity and Watson's Theorem relate the phases of the form factors  $f$  in exclusive semileptonic  $M \rightarrow \pi$  decay (where  $M \in \{B, D, K\}$ ) to the phase shifts in the elastic  $M\pi \rightarrow M\pi$  scattering amplitudes in the corresponding  $J^P$  and isospin channels. We have

$$\frac{f^+(s+i\epsilon)}{f^+(s-i\epsilon)} = \frac{T(s+i\epsilon)}{T(s-i\epsilon)} = e^{2i\delta(s)}, \quad s > s_{\text{th}} \quad (1.1)$$

where  $s_{\text{th}} = (m_M + m_\pi)^2$  and  $T(s)$  is the scattering amplitude, related to the phase shift  $\delta(s)$  by

$$T(s) = \frac{8\pi i s}{\lambda^{1/2}(s)} (e^{2i\delta(s)} - 1) \quad (1.2)$$

where  $\lambda$  is the usual kinematic function. The (inverse) scattering amplitude, in the appropriate isospin and angular momentum channel, is found from [1, 2]

$$T^{-1}(s) = -\bar{I}_0(s) - \frac{1}{8\pi a \sqrt{s_{\text{th}}}} + \frac{1}{V(s)} - \frac{1}{V(s_{\text{th}})} \quad (1.3)$$

Here,  $V$  is the two-particle irreducible scattering amplitude,  $a$  is the scattering length and  $\bar{I}_0$  is calculated from a one-loop bubble diagram. This description automatically implements elastic unitarity, which is necessary for the phase shift to be extracted from equation (1.2).

For multiple multiple subtractions,  $\{(q_i^2, f_i) : i = 0, \dots, n\}$ , the Omnès result reads

$$f(q^2) = \prod_{j=0}^n f_j^{\alpha_j(q^2)} \times \exp \left\{ I_\delta(q^2; \{q_j^2\}) \prod_{k=0}^n (q^2 - q_k^2) \right\} \quad (1.4)$$

$$I_\delta(q^2; \{q_j^2\}) = \frac{1}{\pi} \int_{s_{\text{th}}}^{+\infty} \frac{ds}{(s - q_0^2) \cdots (s - q_n^2)} \frac{\delta(s)}{s - q^2} \quad (1.5)$$

$$\alpha_j(q^2) = \prod_{k=0, k \neq j}^n \frac{q^2 - q_k^2}{q_j^2 - q_k^2}, \quad \alpha_j(q_j^2) = \delta_{ij}, \quad \sum_{k=0}^n \alpha_k(q^2) = 1 \quad (1.6)$$

One can balance the number of subtractions against knowledge of  $\delta$ . In the first application below we use (one or) two subtractions and form-factor input information to extract the scattering length in the corresponding elastic scattering channels [3]. In the second application we make many subtractions to motivate a simple parametrisation of the form factors for exclusive semileptonic  $B \rightarrow \pi$  decays, allowing the extraction of  $|V_{ub}|$  from lattice form factor results combined with experimental partial branching fraction information [4, 5].

## 2. Elastic $s$ -wave $K\pi$ , $B\pi$ , $D\pi$ and $DK$ scattering lengths

We use lattice calculations of the scalar form factor  $f_0(q^2)$  in exclusive semileptonic decays for input. In the Omnès dispersion relation we use one or two subtractions to retain dependence on the phase shift and apply lowest order chiral perturbation theory (ChPT) or heavy meson chiral perturbation theory (HMChPT) for the two-particle irreducible amplitudes  $V$  needed for equation (1.3). In our fits we can then determine the scattering length,  $m_\pi a$ , and the form factor values,  $f_0$ , at the chosen subtraction points.

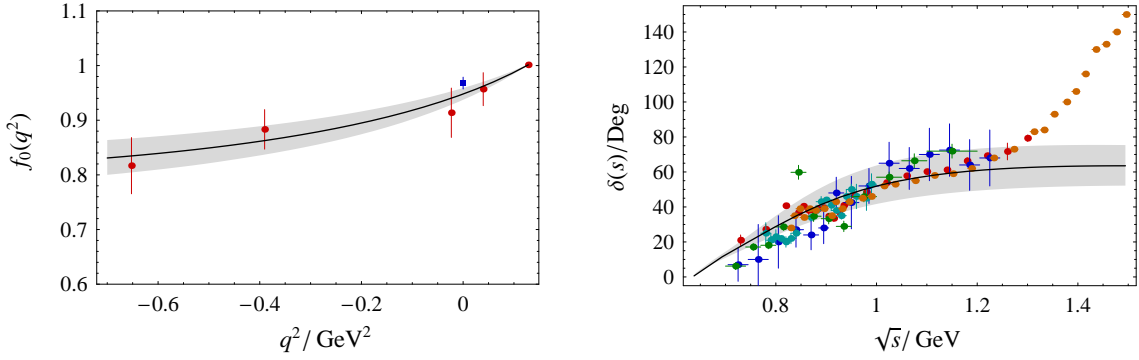


**Figure 1:** The left hand plot shows the  $K_{I3}$  form factor  $f_0(q^2)$ , with a 68% error band, obtained from a fit using a twice-subtracted Omnès relation, implementing a linear relation between  $f_0(0)$  and the scattering length as described in the text. Red points are the form-factor inputs and the blue square shows the result from [6] for  $f_0(0)$  (not fitted). The right hand plot shows the isospin-1/2  $K\pi$   $s$ -wave phase shift with a 68% error band (grey). The phase shift plot also shows experimental data points from [7–11].

## 2.1 Elastic $s$ -wave $K\pi$ scattering

For the isospin-1/2 scalar  $K\pi$  channel, the lowest order ChPT expression for  $V$  is (with  $f_\pi = 92.4\text{MeV}$ )

$$V(s) = \frac{1}{4f_\pi^2} \left( m_K^2 + m_\pi^2 - \frac{5}{2}s + \frac{3}{2s}(m_K^2 - m_\pi^2)^2 \right). \quad (2.1)$$

We take calculated values of the scalar form factor for  $K_{I3}$  decays from  $N_f = 2$  domain wall fermion results by RBC [6]. Since this reference does not provide chirally-extrapolated values for the form factor except at  $q^2 = 0$ , we perform our own simple chiral extrapolation, as described in [3], to provide input pairs  $(q^2, f_0(q^2))$ . To reduce the dependence on the phase shift at large values of the centre-of-mass energy while retaining sensitivity to the scattering length, we use subtraction points at  $q^2 = 0$  and  $q_1^2 = -0.75\text{GeV}^2$ . Our two-subtraction fit shows almost complete anticorrelation of  $f_0(0)$  and the scattering length  $m_\pi a$ , so we redo our fit, implementing a linear relation between them as a constraint (we deduce the relation from a single-subtraction fit)<sup>1</sup>. Our results are:

$$f_0(q_1^2) = 0.827(32), \quad f_0(0) = 0.948(10), \quad m_\pi a = 0.179(17) \quad (2.2)$$

and our fitted form factor and phase shift are shown in Figure 1. The phase-shift plot also shows experimental points for comparison: we emphasise that we have not fit these data, so the agreement with the phase shift determined from a lattice calculation is very encouraging. Since the Omnès integration reaches values where massive resonance exchanges could be relevant, we estimate the associated uncertainties by incorporating the exchange of  $\rho$  and  $K^*$  resonances as well as nonet scalar mesons with masses above 1 GeV, using the isospin-1/2  $K\pi$  scattering amplitude from [12]. This also incorporates some next-to-leading ChPT effects. We find no appreciable changes in the fitted form-factor values, while the scattering length increases by 6%. We have also examined  $K\eta$  coupled-channel effects finding again no appreciable changes in the form-factor values and this

<sup>1</sup>The anticorrelation is not unexpected because the lowest order ChPT expressions for  $f_0(0)$  and the scattering length are linearly related, depending only on  $1/f_\pi^2$  (apart from masses).

time a decrease of up to 5% in the scattering length. Combining these effects, we ascribe an 8% systematic error to the scattering length, leading to a result:

$$m_\pi a = 0.179(17)(14). \quad (2.3)$$

## 2.2 Elastic $s$ -wave $B\pi$ scattering

For the two-particle irreducible isospin-1/2  $s$ -wave  $B\pi$  scattering amplitude we use the leading contact term from the heavy meson chiral perturbation theory (HMChPT) lagrangian [13],

$$V(s) = \frac{1}{4f_\pi^2} \left( 2(m_B^2 + m_\pi^2) - 3s + \frac{(m_B^2 - m_\pi^2)^2}{s} \right). \quad (2.4)$$

We have not included a contribution from the  $t$ -channel  $B^*$ -exchange diagram depending on the leading HMChPT  $B^*B\pi$  interaction term, since this vanishes at  $s_{\text{th}}$  and has magnitude less than 1% of that from the expression above over a large range of  $s$ .

We take input scalar form factor values from the lattice QCD calculations by the HPQCD [14] and FNAL [15] collaborations, assuming that the statistical errors are uncorrelated, while the systematic errors are fully-correlated. Note that the HPQCD results are updated from those we used in [3], while we have also added points read off Figure 7 in [15]. We also use the lightcone sum rule result for  $f_0(0) = f_+(0)$  from [16].

We use two subtraction points at  $q^2 = 0$  and  $q_{\text{max}}^2 = (m_B - m_\pi)^2$  and thus perform a three-parameter fit to  $f_0(0)$ ,  $f_0(q_{\text{max}}^2)$  and the scattering length  $m_\pi a$ . We find

$$f_0(0) = 0.257(31), \quad f_0(q_{\text{max}}^2) = 1.18(21), \quad m_\pi a = 0.32(29). \quad (2.5)$$

The fitted form factor and phase shift are shown in Figure 2. We observe that the fitted value for  $f_0(q_{\text{max}}^2)$  agrees within errors with the heavy quark effective theory prediction in the soft-pion limit [17],  $f_0(m_B^2) = f_B/f_\pi + \mathcal{O}(1/m_b^2) \approx 1.4(2)$  (using  $f_B = 189(27)$  MeV [18]). Our central phase-shift curve shows evidence for a resonance at  $\sqrt{s} \approx 5.6$  GeV, although we cannot give an upper bound for the resonance mass.

## 2.3 Elastic $s$ -wave $D\pi$ and $DK$ scattering

To discuss the  $D\pi$  phase shift we use equation (2.4) with the obvious replacement  $m_B \rightarrow m_D$ . For the  $DK$  phase shift we project into the isospin zero channel, where the two-particle irreducible amplitude again takes the same form with the appropriate substitutions of masses and the replacement  $f_\pi \rightarrow f_K \approx 110$  MeV.

We take input scalar form factor values from the Fermilab-MILC-HPQCD lattice QCD calculation of reference [19]. The chiral extrapolation procedure adopted there leads to parameters for a Becirevic-Kaidalov (BK) [20] parametrisation of  $f_0(q^2)$ , and hence an explicit functional form, rather than values at a set of  $q^2$  points. We therefore generate a toy Monte Carlo ensemble of BK parameters and minimise the integrated squared-difference of the BK fit-function and a twice-subtracted Omnès fit function to determine  $f_0(0)$ ,  $f_0(q_{\text{max}}^2)$  and the scattering length. We note that this fit could be avoided by using the Omnès parametrisation throughout the analysis of the lattice data.

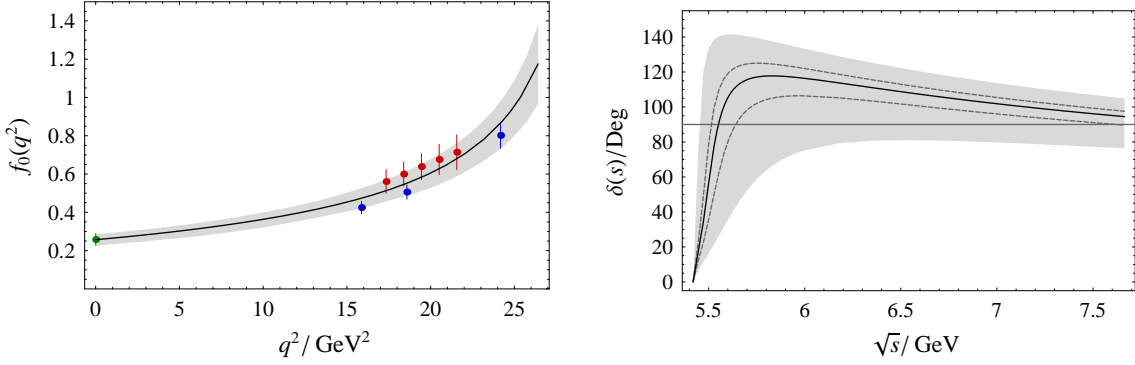


**Figure 2:**  $B\pi$  isospin-1/2 scalar form factor and phase shift, together with 68% confidence level bounds (grey bands). The points on the form factor plot are the inputs from [14–16]. The dashed curves on the phase shift plot show the effect on the statistical uncertainty of reducing the input errors to 1/4 of their current value. The intercept of the phase shift with the horizontal line at  $90^\circ$  indicates the position of a resonance.

For the  $D\pi$  case, we find a scattering length  $m_\pi a = 0.29(4)$ . The output phase shift shows the existence of an  $I = 1/2$   $s$ -wave resonance at  $2.2(1)$  GeV.

For the  $DK$  case, we find in almost all of our Monte Carlo trials that the scattering length is huge, effectively infinite, telling us that  $\text{Re} T^{-1}(s_{\text{th}}) = 0$  as can be seen from equation (1.3). Hence there should be a resonance at threshold,  $(m_D + m_K)^2 = (2.36 \text{ GeV})^2$ . This can be understood by noting the existence of a  $0^+$  state,  $D_{s0}^+(2317)$ , discovered by Babar [21], which is likely an isoscalar [22]. Neglecting isospin-violating decays to  $D_s^+ \pi^0$ , this state could be considered as an isoscalar  $s$ -wave  $DK$  bound state. In this case, following Levinson’s theorem [23], the phase shift close to threshold has the form  $\pi + pa + \dots$ , where  $p$  is the centre-of-mass three-momentum. Three-parameter fits (two subtractions and  $a$ ) show that the scattering length is effectively zero, so we assume that the phase shift is  $\pi$  over the range where the integrand of the phase-shift integral is significant and obtain an excellent two-parameter fit using two subtractions.

### 3. $|V_{ub}|$ from exclusive semileptonic $B \rightarrow \pi$ decay

For our second application we use an Omnès representation for  $f(q^2) = (m_{B^*}^2 - q^2)f_+(q^2)$  with many subtractions [4, 5] to motivate the fit-function

$$f_+(q^2) = \frac{1}{m_{B^*}^2 - q^2} \prod_{i=0}^n [f_+(s_i)(m_{B^*}^2 - s_i)]^{\alpha_i(q^2)}. \quad (3.1)$$

We include  $f_0$  information with a similar Omnès representation for  $f(q^2) = f_0(q^2)$  and apply the constraint  $f_+(0) = f_0(0)$ . This provides an alternative to parametrisations based on the  $z$ -expansion [24, 25]. Adopting the fit procedure described in [5], we combine experimental binned partial-branching fraction information [26–29] for  $f_+$  (to determine shape) with lattice [14, 15, 30, 31] and LCSR [16] form-factor calculations of  $f_+$  and  $f_0$  (for normalisation and partial shape

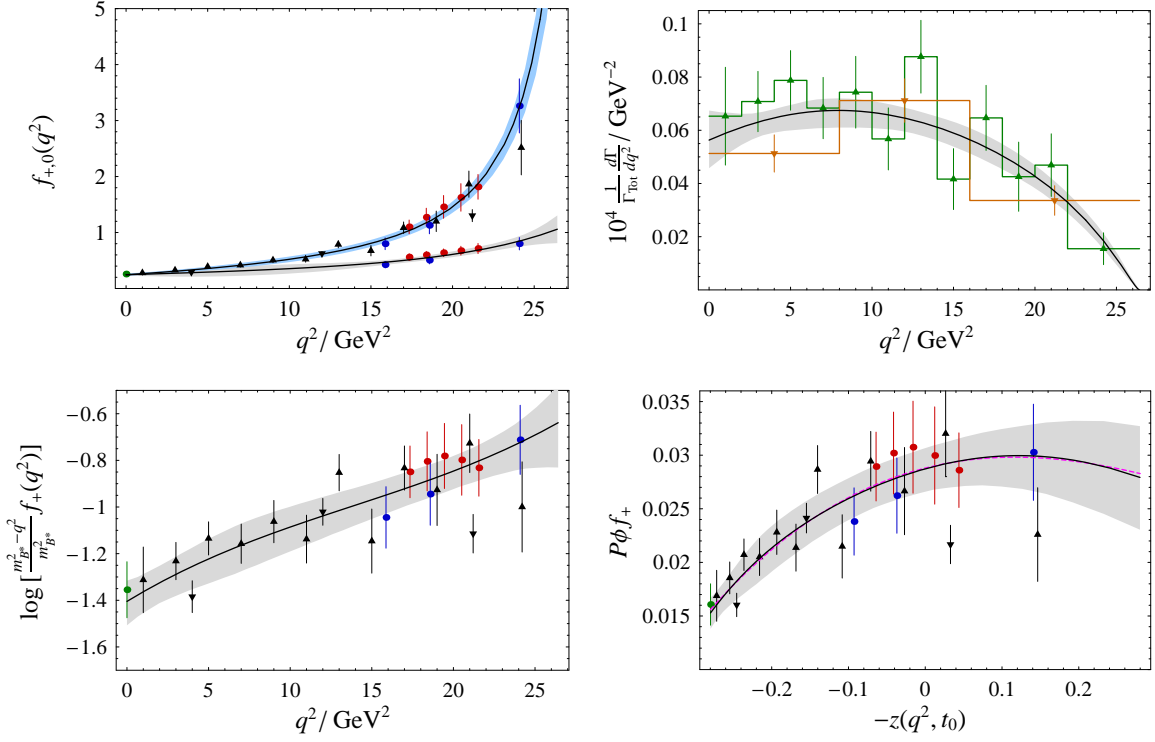


**Figure 3:** Results obtained from the fit to experimental partial branching fraction data and theoretical form factor calculations. The top left plot shows the two form factors with their error bands, the lattice and LCSR input points (dots: green LCSR, red HPQCD, blue FNAL-MILC) and ‘experimental’ points (black triangles, upward-pointing for tagged and downward pointing for untagged data) constructed by plotting at the centre of each bin the constant form factor that would reproduce the partial branching fraction in that bin. The top right plot shows the differential decay rate together with the experimental inputs. The bottom plots provide more details of the inputs and fits by showing on the left  $\log[(m_{B^*}^2 - q^2)/m_{B^*}^2] f_+(q^2)$  as a function of  $q^2$ , and on the right  $P\phi f_+$  as a function of  $-z$  [24, 25]. The dashed magenta curve in the bottom right plot is a cubic polynomial fit in  $z$  to the Omnès curve.

information). From a fit with subtraction points at  $\{0, 1/3, 2/3, 1\}q_{\max}^2$ , we determine:

$$\begin{aligned}
 |V_{ub}| &= (3.47 \pm 0.29) \times 10^{-3} & f_+(q_{\max}^2) &= 7.73 \pm 1.29 \\
 f_+(0) = f_0(0) &= 0.245 \pm 0.023 & f_0(q_{\max}^2/3) &= 0.338 \pm 0.089 \\
 f_+(q_{\max}^2/3) &= 0.475 \pm 0.046 & f_0(2q_{\max}^2/3) &= 0.520 \pm 0.041 \\
 f_+(2q_{\max}^2/3) &= 1.07 \pm 0.08 & f_0(q_{\max}^2) &= 1.06 \pm 0.26
 \end{aligned} \tag{3.2}$$

We also determine the combination  $|V_{ub}|f_+(0) = 8.5(8) \times 10^{-4}$  and the total branching fraction

$$\mathbf{B}(B^0 \rightarrow \pi^- l^+ \nu) = (1.37 \pm 0.08 \pm 0.01) \times 10^{-4} \tag{3.3}$$

where the first uncertainty is from our fit and the second is from the uncertainty in the experimental  $B^0$  lifetime. The result for  $|V_{ub}|$  is in striking agreement with  $|V_{ub}|$  extracted using all other inputs in CKM fits and shows some disagreement with  $|V_{ub}|$  extracted from inclusive semileptonic  $B \rightarrow \pi$  decays. In Figure 3, we show our fitted form factor and differential decay rate distribution.

## References

- [1] J. Nieves and E. Ruiz Arriola, Phys. Lett. B455 (1999) 30, nucl-th/9807035.
- [2] J. Nieves and E. Ruiz Arriola, Nucl. Phys. A679 (2000) 57, hep-ph/9907469.
- [3] J.M. Flynn and J. Nieves, Phys. Rev. D75 (2007) 074024, hep-ph/0703047.
- [4] J.M. Flynn and J. Nieves, Phys. Rev. D76 (2007) 031302, arXiv:0705.3553 [hep-ph].
- [5] J.M. Flynn and J. Nieves, Phys. Lett. B649 (2007) 269, hep-ph/0703284.
- [6] C. Dawson et al., Phys. Rev. D74 (2006) 114502, hep-ph/0607162.
- [7] R. Mercer et al., Nucl. Phys. B32 (1971) 381.
- [8] P. Estabrooks et al., Nucl. Phys. B133 (1978) 490.
- [9] H.H. Bingham et al., Nucl. Phys. B41 (1972) 1.
- [10] S.L. Baker et al., Nucl. Phys. B99 (1975) 211.
- [11] D. Aston et al., Nucl. Phys. B296 (1988) 493.
- [12] M. Jamin, J.A. Oller and A. Pich, Nucl. Phys. B587 (2000) 331, hep-ph/0006045.
- [13] M.B. Wise, Phys. Rev. D45 (1992) 2188.
- [14] E. Dalgic et al., Phys. Rev. D73 (2006) 074502, hep-lat/0601021; erratum ibid D75 (2007) 119906(E).
- [15] M. Okamoto, PoS LAT2005 (2006) 013, hep-lat/0510113.
- [16] P. Ball and R. Zwicky, Phys. Rev. D71 (2005) 014015, hep-ph/0406232.
- [17] G. Burdman, Z. Ligeti, M. Neubert and Y. Nir, Phys. Rev. D49 (1994) 2331, hep-ph/9309272.
- [18] S. Hashimoto, Int. J. Mod. Phys. A20 (2005) 5133, hep-ph/0411126.
- [19] Fermilab Lattice Collaboration, C. Aubin et al., Phys. Rev. Lett. 94 (2005) 011601, hep-ph/0408306.
- [20] D. Becirevic and A.B. Kaidalov, Phys. Lett. B478 (2000) 417, hep-ph/9904490.
- [21] BABAR Collaboration, B. Aubert et al., Phys. Rev. Lett. 90 (2003) 242001, hep-ex/0304021.
- [22] Particle Data Group, W.M. Yao et al., J. Phys. G 33 (2006) 1, <http://pdg.lbl.gov>.
- [23] A.D. Martin and T.D. Spearman, Elementary Particle Theory (North Holland, Amsterdam, 1970) p. 401.
- [24] M.C. Arnesen, B. Grinstein, I.Z. Rothstein and I.W. Stewart, Phys. Rev. Lett. 95 (2005) 071802, hep-ph/0504209.
- [25] T. Becher and R.J. Hill, Phys. Lett. B633 (2006) 61, hep-ph/0509090.
- [26] CLEO Collaboration, S.B. Athar et al., Phys. Rev. D68 (2003) 072003, hep-ex/0304019.
- [27] Belle Collaboration, T. Hokuue et al., Phys. Lett. B648 (2007) 139, hep-ex/0604024.
- [28] BABAR Collaboration, B. Aubert et al., Phys. Rev. Lett. 97 (2006) 211801, hep-ex/0607089.
- [29] BABAR Collaboration, B. Aubert et al., Phys. Rev. Lett. 98 (2007) 091801, hep-ex/0612020.
- [30] Fermilab Lattice, MILC and HPQCD Collaboration, P.B. Mackenzie et al., PoS LAT2005 (2006) 207.
- [31] R.S. Van de Water and P. Mackenzie, PoS LAT2006 (2006) 097.